Transient electromagnetic heating of ceramic slabs with nonlinear thermal transport

C. Nieves[1], A. Baros[1], B. Hoff[1], Z. Cohick[1], J. Perez[2], V. Yakovlev[3], and B. Tilley[3]

2025 IEEE Pulsed Power & Plasma Science (PPPS) | 979-8-3315-4376-1/25/$31.00 ©2025 IEEE | DOI: 10.1109/PPPS56198.2025.11248491

***Abstract*—Our study considers two modeling frameworks for a particular experiment: a 6 mm-thick sample of AlN:Mo, Mo doping either 2% or 4% by volume, is subject to 95 GHz Gaussian electric field at various powers under ambient atmospheric conditions, with the temperature of the sample being observed. The frameworks assume plane electromagnetic (EM) waves normally impeding a thin ceramic slab, whose amplitude varies quasi-steadily on the thermal time scale. The models differ on the assumptions of the thermal profile in the sample: (1) thermal spatial variation, and (2) a spatially uniform temperature. We compare these models with the experiments through a best-fit strategy of the transient temperature evolution; the error between the simulated and experimental data minimized by varying the parameters measuring environmental losses and the applied field magnitude. The results suggest that variations in thermal conductivity and specific heat play a key role in the thermal transport.**

***Index Terms*—electromagnetic heating, power beaming, thermal runaway, mathematical modeling.**

To determine the feasibility of high temperature ceramic composites as susceptors for power beaming applications, experimental evaluation of current modeling frameworks need to be performed with experimentally characterized materials (e.g. [1], [2]). These properties vary both in temperature and in composition, and such variation is typically not included in theoretical or computational modeling (e.g. [3]–[6]). In particular, thermal variations in the loss factor for ceramics can lead to thermal runaway phenomena when microwave EM fields are applied (e.g. [7]). Recent of EM heat exchangers show promising results [5], [6], and the need for experimental confirmation with real materials. This work centers on the EM heating of a material whose specific heat and thermal conductivity depend on temperature.

An $\ell = 6\,$mm-thick sample with a circluar cross-sectional area (radius $L = 25.4\,$mm) of either AlN:Mo 2% or AlN:Mo 4% is subject to $f = 95\,$GHz klystron applied Gaussian electric field (FWHM measured at 15 mm) at powers of $P_o = 18\,$W or $45\,$W under ambient atmospheric conditions, as shown in Fig. 1(a). The distance between the klystron lens and the sample is approximately 330 mm, corresponding to the lens focal length. Temperatures are measured by means of an FLIR camera with data collected at 3-minute intervals, an example of which is given in Fig. 1(b). The average temperature from each image is used as the data to which the fitting parameters are found, as described below.

Support from the US Air Force Office of Scientific Research (AFOSR) awards FA9550-18-1-0528 and FA9550-24-1-0661 is gratefully acknowleged. Approved for public release; distribution is unlimited. AFRL Public Affairs release approval AFRL-2025-4195. The views expressed are those of the author and do not necessarily reflect the official policy or position of the Department of the Air Force, the Department of Defense, or the U.S. Government.

[1]Directed Energy Directorate, Air Force Research Laboratory-Kirtland, Albuquerque, NM, USA

[2]Department of Electrical and Computer Engineering, University of New Mexico, ALbuquerque, NM, USA

[3]Department of Mathematical Sciences, Worcester Polytechnic Institute, Worcester, MA, USA, e-mail: tilley@wpi.edu

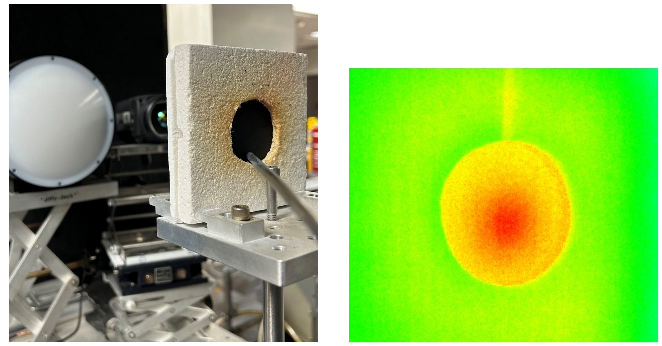

(a) (b)

Fig. 1. (a) Sample (black) in low thermal conductivity hold (white). (b) Sample FLIR heat map at initial field application.

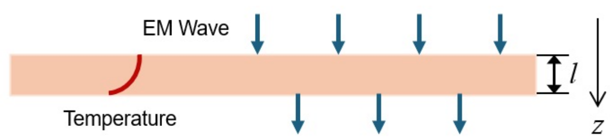

Fig. 2. Coordinate system for forward models.

The two modeling frameworks assume plane EM waves, polarized normal to the frame shown in Fig. 2, normally impeding a thin dielectric composite slab. Thermal losses to the environment normal to the slab boundaries dominate, and the electric field is assumed to be quasi-steady on the thermal time scale. With these assumptions, Gauss's law is satisfied automatically, with Maxwell's equations reduced to a Helmholtz equation for the field amplitude in the slab, which in nondimensional form is

$$\frac{\partial^2 E}{\partial z^2} + \gamma^2\,\epsilon(\theta)\,E \;=\; 0\;,\;\; 0 < z < 1\;, \qquad (1)$$

where $\gamma = \gamma_o\,\ell$ is the dimensionless wavenumber, γ_o the free-space wave number, and $E = E(z,t)$ is the scaled electric field amplitude in the slab. The permitivity $\epsilon(\theta) = \epsilon_r(\theta) + i\,\epsilon_i(\theta)$ depends on the scaled temperature deviation from ambient θ (dimensional temperature $T = 300\,(\theta + 1)$, in units Kelvin). The quantities ϵ_r, ϵ_i are found by applying the nondimensionalization to the dimensional fits found in [8]. We use transmission boundary conditions

$$\underline{z=0}: \qquad \frac{\partial E}{\partial z} + i\gamma E = 2\,i\,\gamma \ , \tag{2}$$

$$\underline{z=1}: \qquad \frac{\partial E}{\partial z} - i\gamma E = 0 \ , \tag{3}$$

to close the EM problem, up to a solution to the unknown θ based on energy conservation in the slab.

The modeling frameworks depend on the assumptions of θ in energy conservation. Our first framework assumes that $\theta = \theta(z,t)$, and both specific heat and thermal conductivity depend on temperature

$$c_p(\theta)\frac{\partial\theta}{\partial t} = \frac{\partial}{\partial z}\left\{k(\theta)\,\frac{\partial\theta}{\partial z}\right\} \quad + \quad P\,\epsilon_i(\theta)|E|^2 \ , \tag{4}$$

where the scaled specific heat c_p and the scaled thermal conductivity k are found by applying the dimensional fits of these quantities for AlN:Mo found in [8]. The power parameter $P = P_o\,(\ell/L)^2\,(2\,f/c\,k_o\,T_o)$, with c being the speed of light, k_o the thermal conductivity at the initial temperature, and $T_o = 300\,\mathrm{K}$, gives a ratio of the applied power to the slab scaled with the characteristic power of conduction. Equation (4) is solved subject to boundary conditions

$$\underline{z=0}: \qquad k(\theta(0,t))\,\frac{\partial\theta}{\partial z} = \mathcal{L}(\theta) \ , \tag{5}$$

$$\underline{z=1}: \qquad k(\theta(1,t))\,\frac{\partial\theta}{\partial z} = -\mathcal{L}(\theta) \ , \tag{6}$$

where conductive flux is balanced by environmental losses $\mathcal{L}(\theta) = B\,\theta + R\left[(\theta+1)^4 - 1\right]$ [6]. The parameters B, R represent the scaled energy losses due to advection and radiation, respectively. We asssume that the initial condition is the uniform dimensional temperature uniform T_i, or

$$\theta(z,0) = \theta_i = \frac{T_i - T_o}{T_o} \ . \tag{7}$$

We call the representation (1)-(7) the *one-dimensional (1D) model*, Our second modeling framework assumes that $\theta = \bar{\theta}(t) = \int_0^1 \theta(z,t)\,dz$, and we formally integrate both sides of (4) over z, and using (5-6), arrive at

$$\begin{aligned} c_p(\bar{\theta})\bar{\theta}'(t) &= P\,\epsilon_i(\bar{\theta})\,||E||^2 - 2\,\mathcal{L}(\bar{\theta}) \ , t > 0 \qquad (8) \\ \bar{\theta}(0) &= \theta_i \ , \qquad (9) \end{aligned}$$

where $||E||^2 = \int_0^1 |E(z,t)|^2\,dz$ with $\theta = \bar{\theta}$. We call this second representation the *thin domain (TD) model*.

Each of these forward problems are solved computationally. For the TD model, (8),(9) are solved computationally using a standard Runge-Kutta method for a given (P, B, R). For the 1D model (1)-(7), θ, E must be solved simultaneously using finite differences in space, Crank-Nicolson in time (vertex-centered mesh for θ and E).

We compare these models indirectly with the experiments through a best-fit strategy to the transient evolution of temperature in the sample. Either the 1D model or the TD model form the forward problem for a given set of (P, B, R), and only these three parameters are varied to fit the spatial average temperature $\int_0^1 \theta dz$ to the data. MATLAB's `fmincon` is used to perform the optimization.

TABLE I
TOTAL RMS ERROR (IN KELVIN)

RMS error	1D Model		TD Model	
	18 W	45 W	18 W	45 W
Mo 2%	0.5910	1.6548	0.5845	1.0946
Mo 4%	0.6801	0.5154	0.6384	0.6507

TABLE II
RELATIVE FIT OF POWER P.

P_{fit}/P_{exp}	1D Model		TD Model	
	18 W	45 W	18 W	45 W
Mo 2%	0.2493	0.2716	1.0060	1.1460
Mo 4%	0.3074	0.2742	1.2307	1.1181

However, the values of P found for these fits can vary significantly. Table II shows the values of the fitted value P_{fit} with the value of P evaluated based on the experimental conditions P_{exp}. Agreement between the scheme experiment coincides with $P_{fit}/P_{exp} = 1$. Note that the TD model performs relatively well under this metric, while the 1D model appears to perform poorly.

Most of the 1D model discrepancy can be explained due to the applied Gaussian beam, since the power is applied nonuniformly in the radial direction. Experimentally we estimate the FWHM to be approximately 15 mm, which when used for the Gaussian envelope for $|E|$ in (4) gives that $P_{fit} \approx 0.211\,P_{exp}$. Since radial transport out of the sample appears to be minimal, the TD model effectively is fitting the average sample temperature.

REFERENCES

[1] B. Hoff, S. Hayden, M. Hilario, R. Grudt, F. Dynys, A. Baros, I. Rittersdorf, and M. Ostraat, "Characterization of AlN-based ceramic composites for use as millimeter wave susceptor materials at high temperature: Dielectric properties of AlN:Mo with 0.25 vol. % to 4.0 vol. % Mo from 25° to 550° C," *J. Mater. Res.*, vol. 34, no. 15, pp. 2573–2581, 2019.

[2] B. Hoff, F. Dynys, S. Hayden, R. Grudt, M. Hilario, A. Baros, and M. Ostraat, "Characterization of AlN-based ceramic composites for use as millimeter wave susceptor materials at high temperature: High temperature thermal properties of AlN:Mo with 0.25% to 4.0% by volume," *MRS Advances*, vol. 4, pp. 1531–1542, 2019.

[3] G. Kriegsmann, M. Brodwin, and D. Watters, "Microwave heating of a ceramic halfspace," *SIAM J. Appl. Math.*, vol. 50, no. 4, pp. 1088–1098, 1990.

[4] G. Kriegsmann, "Thermal runaway in microwave heated ceramics: a one-dimensional model," *J. Appl. Phys.*, vol. 71, no. 4, pp. 1960–1966, 1992.

[5] J. Gaone, B. Tilley, and V. Yakovlev, "Permittivity-based control of thermal runaway in a triple-layer laminate," in *2017 IEEE MTT-S International Microwave Symposium (IMS)*. IEEE, 2017, pp. 459–462.

[6] ——, "Electromagnetic heating control via high-frequency resonance of a triple-layer laminate," *J. Eng. Math.*, vol. 114, no. 1, pp. 65–86, 2019.

[7] V. Yakovlev, S. Allan, M. Fall, and H. Shulman, "Computational study of thermal runaway in microwave processing of zirconia," in *Microwave and RF Power Applications*, J. Tao, Ed. Cépaduès Éditions Toulouse, France, 2011, pp. 303–306.

[8] P. Kumi, S. Martin, V. Yakovlev, M. Hilario, B. Hoff, and I. Rittersdorf, "Electromagnetic-thermal model of a millimeter-wave heat exchanger based on an AlN:Mo susceptor," *COMPEL*, vol. 39, no. 2, pp. 481–496, 2020.